OPEN ACCESS Freely available online

PLOS ONE

Effects of Atrial Natriuretic Peptide on Bicarbonate Transport in Long- and Short-Looped Medullary Thick Ascending Limbs of Rats

Hiroshi Nonoguchi[1]*, Yuichiro Izumi[2], Yushi Nakayama[3], Takanobu Matsuzaki[4], Yukiko Yasuoka[5], Takeaki Inoue[3], Hideki Inoue[3], Tomohiko Mouri[3], Katsumasa Kawahara[5], Hideyuki Saito[4], Kimio Tomita[3]

1 Department of Internal Medicine and Education & Research Center, Kitasato University Medical Center, Kitamoto, Saitama, Japan, **2** Systems Biology Center, National Heart, Lung and Blood Institute, National Institutes of Health, Bethesda, Maryland, United States of America, **3** Department of Nephrology, Kumamoto University Graduate School of Medical Sciences, Kumamoto, Kumamoto, Japan, **4** Department of Pharmacy, Kumamoto University Hospital, Kumamoto, Kumamoto, Japan, **5** Department of Physiology, Kitasato University School of Medicine, Sagamihara, Kanagawa, Japan

Abstract

Atrial natriuretic peptide (ANP) is known to influence NaCl transport in the medullary thick ascending limbs (MAL), where the largest NaCl reabsorption occurs among distal nephron segments in response to arginine vasopressin (AVP). In the present study, we investigated the effect of ANP on bicarbonate (HCO_3^-) transport in the MAL using an isolated tubule perfusion technique. The HCO_3^- concentration was measured using free-flow ultramicro-fluorometer. We first observed basal HCO_3^- reabsorption in both long- and short-looped MALs (lMALs, and sMALs, respectively). AVP inhibited HCO_3^- reabsorption in both lMALs and sMALs, whereas ANP did not change HCO_3^- transport. However, in the presence of AVP, ANP restored the HCO_3^- reabsorption inhibited by AVP both in lMAL and sMAL. The effects of ANP on HCO_3^- transport was mimicked by cyclic GMP. The mRNA expression level of the vasopressin V2 receptor in lMALs was significantly higher than in sMALs, whereas expression of the V1a receptor was unchanged. In summary, AVP inhibits HCO_3^- transport, and ANP counteracts the action of AVP on HCO_3^- transport both in lMALs and sMALs.

Citation: Nonoguchi H, Izumi Y, Nakayama Y, Matsuzaki T, Yasuoka Y, et al. (2013) Effects of Atrial Natriuretic Peptide on Bicarbonate Transport in Long- and Short-Looped Medullary Thick Ascending Limbs of Rats. PLoS ONE 8(12): e83146. doi:10.1371/journal.pone.0083146

Editor: Robert A. Fenton, Aarhus University, Denmark

Received August 10, 2013; **Accepted** October 30, 2013; **Published** December 23, 2013

Funding: This study was supported by Grants-in-Aid for Scientific Research from the Ministry of Education, Culture, Sports, Science and Technology of Japan (21591034, 21591064, 24591244) and by the Science Research Promotion Fund from the promotion and Mutual Aid Corporation for Private Schools of Japan. The funders had no role in study design, data collection and analysis, decision to publish, or preparation of the manuscript.

Competing Interests: The authors have declared that no competing interests exist.

* E-mail: nono@insti.kitasato-u.ac.jp

Introduction

Arginine vasopressin (AVP) plays a central role in urine concentration and dilution by the kidney [1–3]. AVP is known to stimulate NaCl reabsorption in the medullary thick ascending limbs (MAL) where AVP-stimulated Cl reabsorption is highest among the distal nephron segments [4–8]. Because water is not absorbed in MALs, they are considered a diluting segment [5,6,9]. There are two types of nephrons: long- and short-looped nephrons [9,10], which are classified according to their long- and short-looped MALs (lMALs and sMALs, respectively). The functional differences between lMALs and sMALs are not well known [10,11]. The proportion of lMALs and sMALs differs among animals [10]. Humans have a larger number of sMALs than lMALs. In contrast, rats and mice have a larger number of lMALs than sMALs. The pocket mouse has a 10-fold higher single-nephron glomerular filtration rate via long-looped nephrons compared with short-looped nephrons. We have previously shown that AVP-stimulated NaCl reabsorption occurs only in lMALs not in sMALs [11]. It appears that lMALs have a more important role in urine concentration than do sMALs [10].

The kidney plays a major role in not only NaCl and water reabsorption but also in acid excretion [12]. Acid excretion by the kidney consists of bicarbonate (HCO_3^-) reabsorption along the whole nephron and ammonia and titratable acid excretion in the distal nephron. The MAL has a large HCO_3^- absorptive ability and AVP inhibits this abikity [13–18]. The effect of AVP on Cl transport is different between lMALs and sMALs, suggesting heterogeneity of NKCC2 in lMALs and sMALs [11]. However, it is not known whether the effects of AVP on HCO_3^- transport are different between lMALs and sMALs.

Intravenous administration of atrial natriuretic peptide (ANP) is also known to increase NaCl excretion by stimulating guanylate cyclase dependent-cGMP accumulation across almost all nephron segments [19–21]. We have previously shown that ANP counteracts the stimulatory effect of AVP on Cl^- reabsorption in lMALs but not in sMALs [11]. However, it is not known whether ANP influences HCO_3^- transport in lMALs and sMALs.

The aim of our study was to investigate the effects of AVP and ANP on HCO_3^- transport in lMALs and sMALs. We also examined the mRNA expressions of vasopressin V1a and V2 receptors in lMALs and sMALs using real-time PCR.

Methods

Ethics Statement

The protocols for all of the animal experiments were reviewed and approved by the Committee for Animal Experiments at Kitasato University Medical Center (25-2) and Kumamoto University Graduate School of Medical Sciences (18-059, 19-063).

Microperfusion of lMALs and sMALs

Both lMALs and sMALs were dissected from male pathogen-free Sprague-Dawley rats weighing 60–100 g as previously described [11]. In brief, an lMAL was confirmed by the attachment of a thin ascending limb from the inner medulla. A sMAL was thicker than an lMAL and was confirmed by the attachment of a thin descending limb, which comes from the outer stripe of the outer medulla. A lMAL has a straight end whereas a sMAL has a rounded end. Only one tubule (lMAL or sMAL) was obtained from one rat considering the viability of the tubules. Thus the sample number *n* indicates the number of perfused tubules and rats used. The dissection solution had the following composition (in mM): 130 NaCl, 5 KCl, 1 NaH_2PO_4, 1 $MgSO_4$, 1 Ca lactate, 2 Na acetate, 5.5 glucose, 5 L-alanine, 2 L-leucine, 10 HEPES; the pH was adjusted to 7.4 by adding NaOH (final composition: Na^+ 133, K^+ 5, Cl^- 135, Ca^{2+} 1, Mg^{2+} 1, $H_2PO_4^-$ 1, SO_4^{2-} 1, lactate$^-$ 1, acetate$^-$ 2, alanine$^-$ 5, leucine$^-$ 2, glucose 5.5, HEPEs 10).

To examine the effects of AVP or ANP on thetransepithelial potential difference (PD) and HCO_3^- reabsorption, the tubule was washed for at least 20–30 min after starting microperfusion to remove intrinsic AVP. After two to three control collections were performed, AVP or ANP was added to the bath solution. From two to five experimental collections were started after 15 min, and then the AVP or ANP was removed from the bath. From two to four recovery collections were made after 20 min of washout.

To examine the effects of ANP in the presence of AVP, AVP was added to the bath from the beginning. Control collections were made 30 min after the start of the perfusion. Then, ANP was added to the bath and experimental collections were performed after 15 min. Recovery collections were made 20 min after the washout of ANP.

The perfusion solution and the bath solution were identical and the following composition (in mM): 118 NaCl, 25 $NaHCO_3$, 2.5 K_2HPO_4, 1 $MgSO_4$, 1 Ca lactate, 2 Na acetate, 5.5 glucose, 5 L-alanine, 2 L-leucine (final composition: Na^+ 145, K^+ 5, Cl^- 118, Ca^{2+} 1, HCO_3^- 25, HPO_4^{2-} 2.5, SO_4^{2-} 1, acetate$^-$ 2, alanine$^-$ 5, leucine$^-$ 2, glucose 5.5). The solution was continuously gassed with 5% CO_2-95% O_2.

Measurement of PD and HCO_3^-

The PD was continuously measured using calomel electrodes and agarose bridges (0.16 M NaCl). Agarose bridges were connected to the end of the perfusion pipette (perfusate) and the bath. The total CO_2 concentration is the sum of the bicarbonate, carbonate and dissolved CO_2 levels. Because the dissolved CO_2 is very small in amount, the bicarbonate concentration can be considered the total CO_2 concentration. The HCO_3^- concentrations in perfusate, bath, and collected fluid were measured using free-flow ultramicro-fluorometer as described previously [22]. The reagent for the determination of T_{CO2} (Sigma 130-UV) was protected from T_{CO2} in the air with oil at the injection port and CO_2 absorber (Ascarite II, Thomas Scientific, NJ) behind the reservoir of the reagent. The otal CO_2 concentration in the perfusate was repeatedly measured during the experiments to check the stability of the solution. Because there was no fluid transport in the lMAL and sMAL as we reported previously, the net bicarbonate transport (J T_{CO2}) was calculated as J $T_{CO2} = (C_O\text{-}C_L)V_L/L$, where C_O and C_L are the HCO_3^- concentration in the collected fluid and perfusate, respectively, V_L is the rate at which fluid is collected at the end of the tubule, and L is the tubule length. The perfusate and bath solutions were continuously babbled with 95% O_2 - 5% CO_2. The tubules were perfused by identical perfusate and bath solutions. Because dissolved CO_2 is very small in amount and the viability of the perfused tubules was checked against the PD, any leak of CO_2 from the cell membrane can be ruled out. Because we could measure bicarbonate transport and the values were very close to the values reported by Good et al., we considered that our measurements of the bicarbonate would be accurate. To avoid CO_2 loss into the mineral oil in the collection pipette, the mineral oil was water-saturated, and the water was bubbled with 95% O_2 - 5% CO_2 before the experiments.

Real-time PCR with microdissected nephron segments

Isolation of mRNA from the renal tubules and reverse transcription were performed as described previously [23,24]. sMAL and lMAL were dissected as described above from control rats after 30 min incubation of kidney slices at 37°C in the 0.1% collagenase solution in the presence of vanadyl ribonucleoside complex (VRC). We performed a TaqMan quantitative real-time RT-PCR using an ABI PRISM 7900 sequence detection system (Applied Biosystems, CA, USA) to determine the mRNA expression level of rat V1a receptor (V1aR) and V2 receptor (V2R) and eukaryotic 18S rRNA. The following TaqMan 18S rRNA control reagents and products for TaqMan gene expression assays were purchased from Applied Biosystems: rat V1aR, Rn00583910_m1; rat V2R, Rn00569508_g1; and 18S rRNA, 4319413E. To quantify the mRNA expression level for V1aR, V2R and 18s rRNA, relative standard curves were prepared using diluted cDNA from the outer medulla of rat kidney in triplicate (dynamic range, 1 to 1024-fold; 4-fold serial dilution). The slopes and R2 values of standard curve for V1aR, V2R and 18S rRNA were -3.346, -3.354 and -3.493, and 0.9984, 0.9993 and 0.9992, respectively. The amounts of V1aR and V2R were normalized to the amount of 18S rRNA.

Statistics

Between two to five measurements were averaged to obtain a single value for each experimental condition in each tubule. The results were expressed as the mean ±SE. Student's *t* test or analysis of variance followed by the multiple comparison of Dunnet was employed for statistical analysis. Statistical significance was obtained at $p<0.05$. Dr. SPSS-II (Tokyo) was used for the analysis.

Results

Effects of AVP and ANP on PD and J T_{CO2} in lMALs and sMALs

We previously reported that AVP stimulated the PD in lMALs but not in sMAL. Our present data confirmed the effect of AVP on the PD. AVP increased the PD in lMALs, but it did not change the PD in sMAL. Time course of the basal condition showed no change in the PD in lMALs and a decrease in sMALs (Figs. 1 and 2 and Series 1 and 2 in Table 1). Time course experiments on the basal condition showed no change in HCO_3^- reabsorption either in lMALs and sMALs (Fig. 2 and Series 2 in Table 1). AVP at a concentration of 10^{-10} M inhibited HCO_3^- reabsorption both in

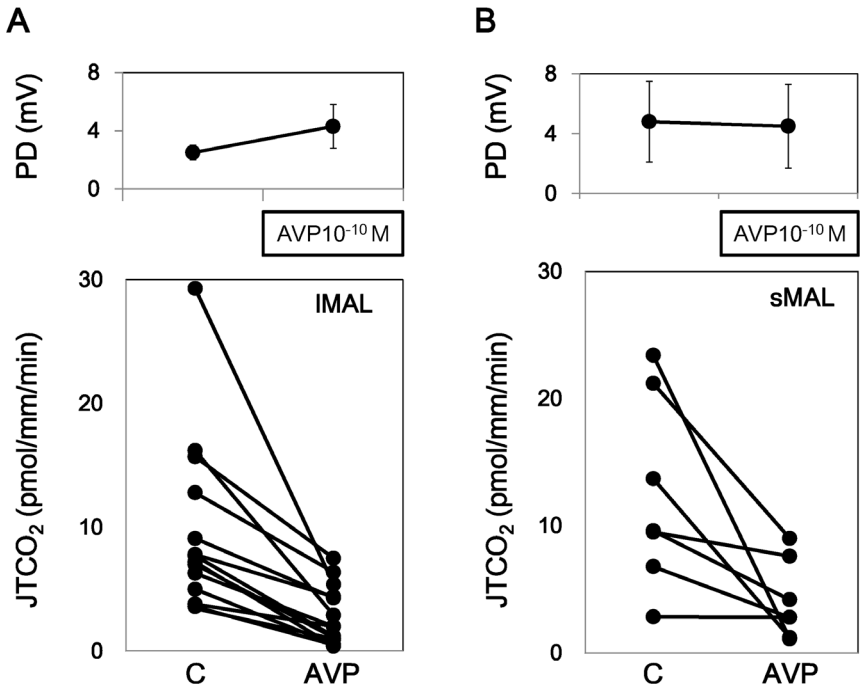

Figure 1. Effects of AVP on HCO_3^- transport in lMAL and sMAL. The addition of 10^{-10} M AVP to the bath decreased HCO_3^- absorption both in lMALs and sMALs, but the PD increased only in lMALs.
doi:10.1371/journal.pone.0083146.g001

lMALs and in sMALs (Fig. 1 and Series 1 in Table 1). These data are compatible with the report by Good et al. [13,14].

In contrast, ANP alone had no effect on HCO_3^- transport in lMALs (Fig. 3 and Series 3 in Table 1).

Effects of ANP and cGMP on the presence of AVP in lMALs and sMALs

Next, the effect of ANP was examined in the presence of AVP. AVP at a concentration of 10^{-10} M was present in the bath

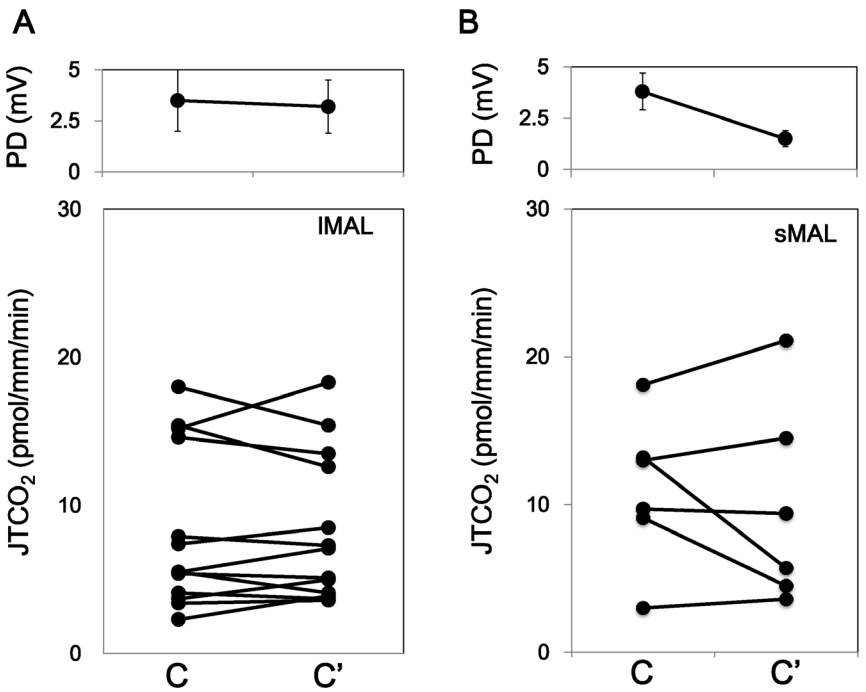

Figure 2. Time course of HCO_3^- transport in lMAL and sMAL. Vehicle was added to the bath after the collection durng the control period. HCO_3^- transport was stable with time both in lMALs and sMALs, although the PD was decreased only in sMALs.
doi:10.1371/journal.pone.0083146.g002

Table 1. Effects of AVP, ANP and cGMP on HCO_3^- transport in sMALs and lMALs.

	L (mm)	$[TCO_2]p$ (mM)		NCR (nl/mm/min)	$[TCO_2]c$ (mM)	J_{TCO2} (pmol/mm/min)	PD (mV)
Series 1 (C = control, E = 10^{-10}M AVP)							
lMAL (n = 13)	0.63±0.10	23.7±1.0	C	2.68±0.47	19.4±1.0	9.6±1.9	2.5±0.5
			E	1.93±0.29	21.9±1.1	2.9±0.6*	4.3±1.5*
sMAL (n = 7)	0.71±0.08	26.3±0.6	C	2.85±0.64	21.3±0.7	12.4±2.6	4.8±2.7
			E	2.31±0.33	24.1±0.7	4.1±1.1*	4.5±2.8
Series 2 (C = control, E = control)							
lMAL (n = 13)	0.72±0.08	23.9±1.1	C	3.08±0.68	20.2±1.0	8.3±1.5	3.5±1.5
			E	2.13±0.24	19.8±1.0	8.3±1.4	3.2±1.3
sMAL (n = 6)	0.61±0.11	26.3±0.7	C	2.12±0.42	20.4±1.0	11.0±2.1	3.8±0.9
			E	1.99±0.38	21.1±0.4	9.8±2.5	1.5±0.4*
Series 3 (C, C′ = control, E = 10^{-8}M AVP)							
lMAL (n = 7)	0.63±0.07	27.9±0.4	C	3.06±0.42	23.6±0.7	12.1±3.6	2.5±0.3
			E	2.56±0.27	24.8±1.0	8.3±3.0	1.8±0.3*
			C′	2.30±0.39	23.9±0.9	8.1±3.5	1.7±0.4*
Series 4 (C, C′ = 10^{-10}M AVP, E = 10^{-10}M AVP+10^{-8}M ANP)							
lMAL (n = 8)	0.72±0.09	22.5±1.0	C	1.57±0.30	20.5±1.0	2.2±0.4	2.4±0.6
			E	1.90±0.45	19.3±0.9	4.7±0.7*	1.8±0.5*
			C′	1.40±0.14	20.0±1.1	2.6±0.6	1.6±0.5*
sMAL (n = 3)	0.69±0.08	27.5±0.1	C	2.77±0.39	26.4±0.3	2.5±0.6	2.7±0.2
			E	2.92±0.41	26.3±0.2	4.4±0.1*	1.9±0.2*
			C′	2.84±0.06	26.8±0.2	1.9±0.7	1.0±0.3*
Series 5 (C, C′ = 10^{-10}M AVP, E = 10^{-10}M AVP+10^{-10}M ANP)							
lMAL (n = 8)	0.66±0.06	26.8±0.6	C	2.19±0.25	24.4±0.9	3.6±0.7	2.5±1.5
			E	3.21±0.41	24.4±0.7	6.5±0.8*	2.0±1.3
			C′	2.68±0.42	25.8±0.5	3.4±1.0	0.5±0.1*
Series 6 (C, C′ = 10^{-10}M AVP, E = 10^{-10}M AVP+10^{-4}M cGMP)							
lMAL (n = 5)	0.58±0.09	26.6±0.8	C	2.22±0.58	24.0±0.4	4.0±0.3	1.7±0.8
			E	2.47±0.39	23.8±0.7	5.6±0.4*	1.1±0.7*
			C′	3.29±1.32	25.4±0.7	2.9±0.6	0.6±0.2

Values are mean ± SE. Abbreviations: L, tubular length; C, control period; E, experimental period; C′, recovery period; $[T_{CO2}]_p$, total CO_2 concentration in perfusate and bath; $[T_{CO2}]_c$, total CO_2 concentration in the collected solution; JTCO2, net bicarbonate absorption, NCR, normalized collection rate; PD, transepitherial potential difference;

*$p<0.05$ vs. control period.

doi:10.1371/journal.pone.0083146.t001

throughout the experiment. ANP at a concentration of 10^{-8} M reversibly stimulated J T_{CO2} in lMAL (Fig. 4B and Series 5 in Table 1). The effects of low doses of ANP (10^{-10} M) and cGMP (10^{-4} M) were examined in lMALs. ANP at a concentration of 10^{-10} M also reversibly stimulated AVP-inhibited J T_{CO2} (Fig. 4A and Series 4 in Table 1). cGMP at a concentration of 10^{-4} M mimicked the effect of ANP on J T_{CO2} (Fig. 4C and Series 6 in Table 1).

ANP at a concentration of 10^{-8} M also reversibly stimulated J T_{CO2} in sMALs (Fig. 5 and Series 4 in Table 1).

mRNA expression levels of vasopressin V1a and V2 receptors

The expression levels of V1aR and V2R in lMALs and sMALs were examined using real time PCR. V2R mRNA expression in lMALs was significantly higher than in sMALs (1.38±0.11* and 1.00±0.02 in lMALs and sMALs, respectively, n = 5, * $p<0.05$ vs. sMAL, Fig. 6). In contrast, V1aR mRNA expression was not significantly different between in lMALs and sMALs (0.82±0.28 and 1.00±0.24 in lMAL and sMAL, respectively, n = 3–4). The V2R/V1aR ratio in lMALs was higher than sMALs (1.7 and 1.0, in lMAL and sMAL, respectively, Fig. 6). To confirm the absence of possible contamination by outer medullary collecting ducts (OMCDs) in lMALs and sMALs, the V2R mRNA expression level was compared in OMCDs, lMALs, and sMALs. The expression of V2R mRNA was 10 times higher in OMCDs (9.60±0.74, n = 5) than in lMALs and sMALs, suggesting highly pure lMAL and sMAL samples.

Discussion

Our data showed that AVP inhibited JT_{CO2} and that ANP counteracted the effect of AVP both in lMALs and sMALs. The effects of AVP and ANP opposed each other in lMALs and sMALs with respect to bicarbonate transport but only in lMALs with respect to chloride transport.

Acid-base regulation is an important role of the kidney alongside water and sodium excretion. Filtered bicarbonate from

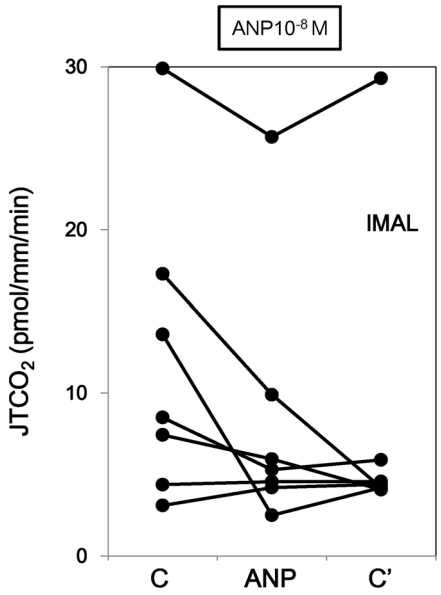

Figure 3. Effect of ANP on HCO_3^- transport in IMALs in the absence of AVP. ANP at the concentration of 10^{-8} M did not cause changes in HCO_3^- absorption in IMALs in the absence of AVP.
doi:10.1371/journal.pone.0083146.g003

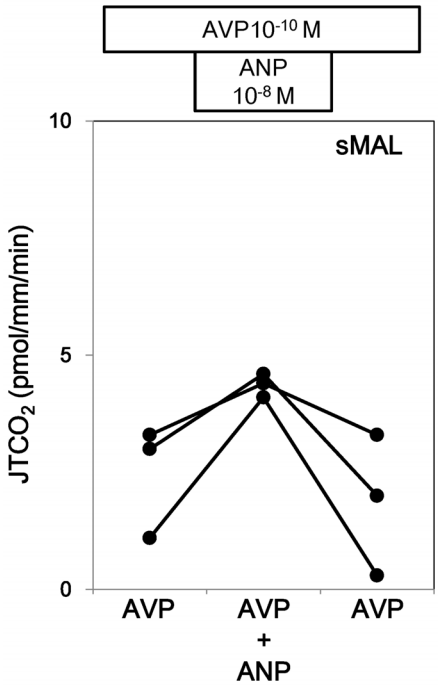

Figure 5. Effect of ANP on HCO_3^- transport in the presence of AVP in sMALs. ANP at the concentration of 10^{-8} M stimulated HCO_3^- reabsorption in the presence of 10^{-10} M AVP in sMALs.
doi:10.1371/journal.pone.0083146.g005

the glomerulus is completely reabsorbed by the nephron: 70–85% by proximal tubules, 10–20% by thick ascending limbs, 3–5% by distal convoluted tubules, and 2% by the collecting ducts [12]. HCO_3^- reabsorption in the distal nephron is regulated by vasopressin and aldosterone [1,12–18,25,26]. Because vasopressin and aldosterone are key factors to regulate body fluid, HCO_3^- reabsorption in the MAL should be correlated with the maintenance of body fluid homeostasis. The effect of AVP on HCO_3^- transport is different between the MAL and the collecting duct [12–18,25–27]. AVP inhibits HCO_3^- reabsorption in the MAL, while it stimulates reabsorption in the cortical collecting ducts. HCO_3^- transport in the MAL has been extensively examined by Good and colleagues [13–18]. Vasopressin is known

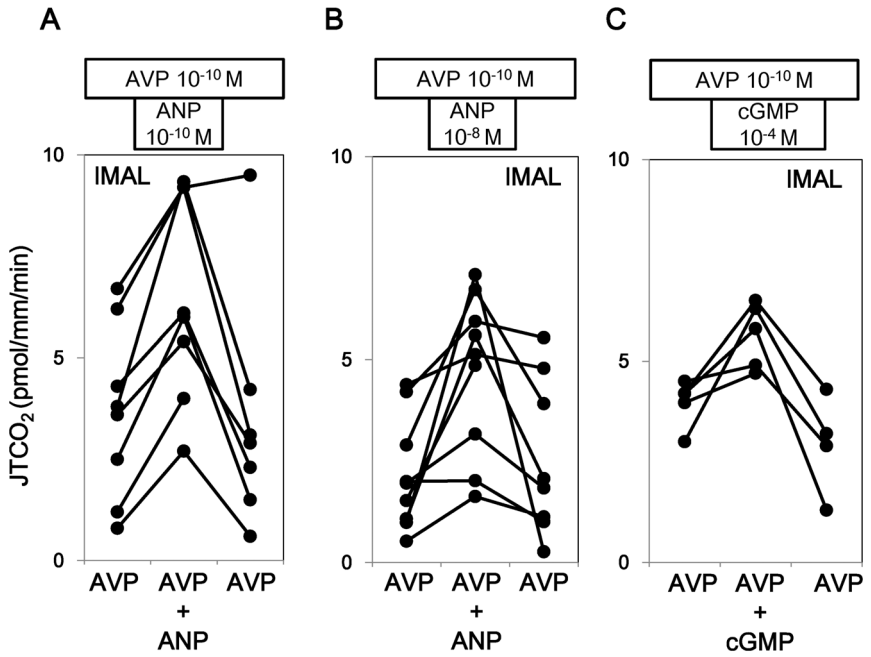

Figure 4. Effects of ANP and cGMP on HCO_3^- transport in the presence of AVP in IMALs. ANP at the concentration of 10^{-10} M and 10^{-8} M significantly increased HCO_3^- reabsorption in the presence of 10^{-10} M AVP in IMALs (A and B, respectively). cGMP at the concentration of 10^{-4} M mimicked the effect of ANP on HCO_3^- transport in the presence of 10^{-10} M AVP in IMALs (C).
doi:10.1371/journal.pone.0083146.g004

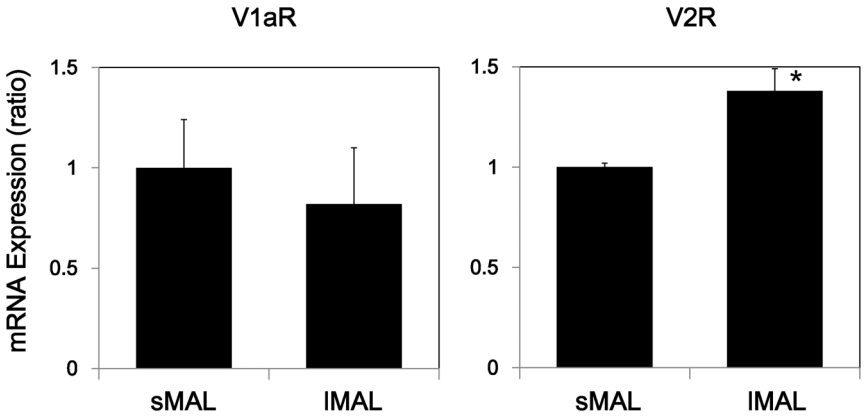

Figure 6. Expression levels of V1aR and V2R mRNA in sMALs and lMALs. The expression levels of V1aR in sMALs and lMALs were examined using real time PCR. sMALs and lMALs were dissected out of control rats after 30 min of incubation of the kidney slices at 37°C in a 0.1% collagenase solution in the presence of VRC. * $p<0.05$ vs. sMAL, n = 3–5.
doi:10.1371/journal.pone.0083146.g006

to inhibit HCO_3^- transport in the MAL by regulating the Na^+/H^+ exchanger, NHE3, in the apical membrane [15,17]. However, Good et al. reported that NHE1 in the basolateral membrane has a major role in basal HCO_3^- transport in the MAL [15,17].

AVP is known to induce NaCl reabsorption via NKCC2 in the MAL [5,6]. We have shown that AVP stimulates Cl^- reabsorption in lMALs but not in sMALs, indicating the different effect of AVP on NKCC2 in lMALs and sMALs [11]. In contrast, HCO_3^- transport in the MAL is not dependent on furosemide-sensitive NaCl reabsorption via NKCC2 [5,27]. Inhibition of HCO_3^- reabsorption by AVP and the counteracting effect of ANP on AVP occur both in lMALs and sMALs to the same degree. Thus, the regulation of HCO_3^- transport and Cl^- transport by AVP and ANP are independent each other. Regulation of HCO_3^- transport by AVP is caused by the activation of the Na-H exchanger (NHE) in the apical and basolateral membranes [15,17,18]. The lack of a difference in HCO_3^- transport between lMALs and sMALs suggests that the NHE in lMALs and sMALs are functionally same, whereas the NKCC2s in lMALs and sMALs are functionally different. It would be interesting to compare the distributions of NKCC2 isoform A, B, and F between lMALs and sMALs.

The diuretic action of ANP is now used clinically. ANP has diuretic and natriuretic effects in various segments of the nephron including the MAL [1,11,19–21,28–32]. The effects of ANP on sodium excretion are mainly caused by the action in the thick ascending limb and collecting duct [1,11,20,21,29–32]. The effects of ANP on glomerular filtration and proximal tubule sodium transport have been less well studied [1,33]. Our data show that ANP participates in the regulation of not only NaCl excretion but also acid-base balance in the MAL. In our experiments, ANP did not have a direct effect on HCO_3^- transport in the MAL. Stimulation of HCO_3^- transport by ANP was observed only in the presence of AVP, suggesting that ANP might inhibit the vasopressin-dependent protein kinase A (PKA) pathway. Vasopressin stimulates cAMP generation and subsequent PKA activity via V2R by activating adenylyl cyclase, while ANP stimulates cGMP generation [19,20,34]. We showed that cGMP mimicked the effects of ANP in the MAL in the presence of AVP. Good et al. have shown that PGE2 stimulates HCO_3^- reabsorption in the presence but not in the absence of AVP [16]. The effects of PGE2 and ANP look the same in terms of their inhibitory effects on the vasopressin-induced decrease in bicarbonate transport. However, the effects of ANP and PGE2 on AVP-dependent cAMP generation are different [11]. We have shown that ANP does not change AVP-dependent cAMP accumulation [21], whereas PGE2 inhibits vasopressin-dependent cAMP generation in the MAL [11]. It is hypothesized that PGE2 inhibits upstream of PKA whereas ANP inhibits downstream of PKA pathway. AVP is known to stimulate the PKC pathway via V1aR in the intercalated cells of the collecting ducts [35]. Activation of PKC by luminal AVP causes a decrease in the AVP-dependent cAMP accumulation in initial inner medullary collecting duct [34]. If ANP stimulates PKC activity, a decrease in AVP-dependent cAMP accumulation would occur. Therefore, the oppositional effect of ANP on AVP action would be PKC independent in the MAL.

Our data showed that lMALs express V2R more than do sMALs. V2R has a major role in the antidiuretic action of AVP and is present in lMALs, sMALs and the principal cells of the collecting ducts [1,34,36]. In contrast, V1aR is present in lMALs, sMALs, and the intercalated cells of the collecting duct and has an important role in V2R-mediated vasopressin effects, including on HCO_3^- transport [1,23,37–40]. How V1aR and V2R participate in HCO_3^- transport in the MAL is not clear yet [1,23,38–40]. In the collecting duct, vasopressin stimulates acid excretion in the intercalated cells by regulating the action of aldosterone [23]. V1aR is essential for the nucleocytoplasmic transport of mineralocorticoid receptor in the intercalated cells [35]. The lack of V1aR causes type 4 renal tubular acidosis [23]. Although mineralocorticoid receptorsare present in the MAL, the nature of interaction between V1aR and mineralocorticoid receptors in the MAL is not yet known [41,42]. Good et al. have reported nongenomic regulation of NHE3 by aldosterone in the MAL [18]. The present study may imply a different mechanism of HCO_3^- transport by AVP in the MAL compared with the collecting duct because both V1aR and V2R are present in a single type of cell in the MAL. The role of V1aR in HCO_3^- transport in the MAL and its interaction with aldosterone and ANP needs to be examined further.

In conclusion, the present study clearly shows that AVP inhibits HCO_3^- reabsorption in both lMALs and sMALs and that ANP counteracts the action of AVPon HCO_3^- reabsorption in both lMALs and sMALs.

Author Contributions

Conceived and designed the experiments: HN YI YN KT. Performed the experiments: HN YI YN TM YY TI HI TM. Analyzed the data: HN YI

TM. Contributed reagents/materials/analysis tools: KK HS KT. Wrote the paper: HN YI.

References

1. Inoue T, Nonoguchi H, Tomita K (2001) Physiological effects of vasopressin and atrial natriuretic peptide in the collecting duct. Cardiovasc Res 51: 470–80.
2. Nielsen S, Frøkiaer J, Marples D, Kwon TH, Agre P, et al. (2002) Aquaporins in the kidney: from molecules to medicine. Physiol Rev 82: 205–44.
3. Sands JM, Layton HE (2009) The physiology of urinary concentration: an update. Semin Nephrol 29: 178–95.
4. Besseghir K, Trimble ME, Stoner L (1986) Action of ADH on isolated medullary thick ascending limb of the Brattleboro rat. Am J Physiol 251 (Renal Fluid Electrolyte Physiol 20): F271–7.
5. Hebert SC, Andreoli TE (1984) Control of NaCl transport in the thick ascending limb. Am J Physiol 246: F745–56.
6. Knepper MA, Kim GH, Fernández-Llama P, Ecelbarger CA (1999) Regulation of thick ascending limb transport by vasopressin. J Am Soc Nephrol 10: 628–34.
7. Wittner M, Di Stefano A (1990) Effects of antidiuretic hormone, parathyroid hormone and glucagon on transepithelial voltage and resistance of the cortical and medullary thick ascending limb of Henle's loop of the mouse nephron. Pfleugers Arch 415: 707–712.
8. Work J, Galla JH, Booker BB, Schafer JA, Luke RG (1985) Effect of ADH on chloride reabsorption in the loop of Henle of Brattleboro rat. Am J Physiol 249 (Renal Fluid Electrolyte Physiol 18): F698–F703.
9. Kriz W (1981) Structural organization of the renal medulla: comparative and functional aspects. Am J Physiol 241: R3–16.
10. Jamison RL (1987) Short and long loop nephrons. Kidney Int 31: 597–605.
11. Nonoguchi H, Tomita K, Marumo F (1992) Effects of atrial natriuretic peptide and vasopressin on chloride transport in long- and short-looped medullary thick ascending limbs. J Clin Invest 90: 349–357.
12. Koeppen BM (2009) The kidney and acid-base regulation. Adv Physiol Educ 33: 275–81.
13. Good DW, Knepper MA, Burg MB (1984) Ammonia and bicarbonate transport by thick ascending limb of rat kidney. Am J Physiol 247: F35–44.
14. Good DW (1990) Inhibition of bicarbonate absorption by peptide hormone and cyclic adenosine monophosphate in rat medullary thick ascending limb. J Clin Invest 85: 1006–1013.
15. Good DW, George T, Watts BA 3rd (1995) Basolateral membrane Na+/H+ exchange enhances HCO3- absorption in rat medullary thick ascending limb: evidence for functional coupling between basolateral and apical membrane Na+/H+ exchangers. Proc Natl Acad Sci USA 92: 12525–9.
16. Good DW (1996) PGE2 reverses AVP inhibition of $HCO3^-$ absorption in rat MTAL by activation of protein kinase C. Am J Physiol 270: F978–85.
17. Good DW, Watts BA 3rd, George T, Meyer JW, Shull GE (2004) Transepithelial $HCO3^-$ absorption is defective in renal thick ascending limbs from Na^+/H^+ exchanger NHE1 null mutant mice. Am J Physiol Renal Physiol 287: F1244–9.
18. Good DW, George T, Watts BA 3rd (2006) Nongenomic regulation by aldosterone of the epithelial NHE3 Na(+)/H(+) exchanger. Am J Physiol Cell Physiol 290: C757–63.
19. Brenner BM, Ballermann BJ, Gunning ME, Zeidel ML (1990) Diverse biological action of atrial natriuretic peptide. Physiol Rev70: 665–699.
20. Knepper MA, Lankford SP, Terada Y (1991) Renal tubular actions of ANF. Can J Physiol Pharmacol 69: 1537–45.
21. Nonoguchi H, Knepper MA, Manganiello VC (1987) Effects of atrial natriuretic factor on cyclic guanosine monophosphate and cyclic adenosine monophosphate accumulation in microdissected nephron segments from rats. J Clin Inves. 79: 500–507.
22. Star RA (1990) Quantitation of total carbon dioxide in nanoliter samples by flow-through fluorometry. Am J Physiol 258: F429–32.
23. Izumi Y, Hori K, Nakayama Y, Kimura M, Hasuike Y, et al. (2011) Aldosterone requires vasopressin V1a receptors on intercalated cells to mediate acid-base homeostasis. J Am Soc Nephrol 22: 673–80.
24. Matsuzaki T, Watanabe H, Yoshitome K, Morisaki T, Hamada A, et al. (2007) Downregulation of organic anion transporters in rat kidney under ischemia/reperfusion-induced acute renal failure. Kidney Int 71: 539–47.
25. Bichara M, Mercier O, Houillier P, Paillard M, Leviel F (1987) Effects of antidiuretic hormone on urinary acidification and on tubular handling of bicarbonate in the rat. J Clin Invest 80: 621–630.
26. Tomita K, Pisano JJ, Burg MB, Knepper MA (1986) Effects of vasopressin and bradykinin on anion transport by the rat cortical collecting duct. Evidence for an electroneutral sodium chloride transport pathway. J Clin Invest 77: 136–41.
27. Capasso G, Unwin R, Agulian S, Giebisch G (1991) Bicarbonate transport along the loop of Henle. I. Microperfusion studies of load and inhibitor sensitivity. J Clin Invest 88: 430–7.
28. Bailly C (2000) Effect of luminal atrial natriuretic peptide on chloride reabsorption in mouse cortical thick ascending limb: inhibition by endothelin. J Am Soc Nephrol11: 1791–7.
29. Light DB, Schwiebert EM, Karlson KH, Stanton BA (1989) Atrial natriuretic peptide inhibits a cation channel in renal inner meduallry collacting duct cells. Science (Wash DC) 243: 383–385.
30. Nonoguchi H, Sands JM, Knepper MA (1988) Atrial natriuretic factor inhibits vasopressin-stimulated osmotic water permeability in rats inner medullary collecting duct. J Clin Invest 82: 1383–1390.
31. Nonoguchi H, Sands JM, Knepper MA (1989) ANF inhibits NaCl and fluid absorption in cortical collecting duct of rat kidney. Am J Physiol 256: F179–86.
32. Zeidel ML, Seifter JL, Brenner BM, Silva P (1986) Atrial peptide inhibits oxygen consumption in kidney medullary collecting duct cells. Am J Physiol 251 (Renal Fluid Electrolyte Physiol 20): F379–F383.
33. Wang W, Li C, Nejsum LN, Li H, Kim SW, et al. (2006) Biphasic effects of ANP infusion in conscious, euvolumic rats: roles of AQP2 and ENaC trafficking. Am J Physiol Renal Physiol 290: F530–41.
34. Nonoguchi H, Owada A, Kobayashi N, Takayama M, Terada Y, et al. (1995) Immunohistochemical localization of V2 vasopressin receptor along the nephron and functional role of luminal V2 receptor in terminal inner medullary collecting ducts. J Clin Invest 96: 1768–78.
35. Hori K, Nagai T, Izumi Y, Kimura M, Hasuike Y, et al. (2012) Vasopressin V1a receptor is required for nucleocytoplasmic transport of mineralocorticoid receptor. Am J Physiol Renal Physiol 303: F1080–8.
36. Machida K, Wakamatsu S, Izumi Y, Yosifovska T, Matsuzaki T, et al. (2007) Downregulation of the V2 vasopressin receptor in dehydration: mechanisms and role of renal prostaglandin synthesis. Am J Physiol Renal Physiol 292: F1274–82.
37. Carmosino M, Brooks HL, Cai Q, Avis LS, Opalenik S, et al. (2007) Axial heterogeneity of vasopressin-receptor subtypes along the human and mouse collecting duct. Am J Physiol Renal Physiol 292: F351–60.
38. Izumi Y, Nakayama Y, Mori T, Miyazaki H, Inoue H, et al. (2007) Downregulation of vasopressin V2 receptor promoter activity via V1a receptor pathway. Am J Physiol Renal Physiol 292: F1418–26.
39. Tashima Y, Kohda Y, Nonoguchi H, Ikebe M, Machida K, et al. (2001) Intranephron localization and regulation of the V1a vasopressin receptor during chronic metabolic acidosis and dehydration in rats. Pfleugers Arch 442: 652–61.
40. Yasuoka Y, Kobayashi M, Sato Y, Zhou M, Abe H, et al. (2013) The intercalated cells of the mouse kidney $OMCD_{is}$ are the target of the vasopressin V1a receptor axis for urinary acidification. Clin Exp Nephrol In press
41. Ackermann D, Gresko N, Carrel M, Loffing-Cueni D, Habermehl D, et al. (2010) In vivo nuclear translocation of mineralocorticoid and glucocorticoid receptors in rat kidney: differential effect of corticosteroids along the distal tubule. Am J Physiol Renal Physiol 299: F1473–85.
42. Todd-Turla KM, Schnermann J, Fejes-Tóth G, Naray-Fejes-Tóth A, Smart A, et al. (1993) Distribution of mineralocorticoid and glucocorticoid receptor mRNA along the nephron. Am J Physiol 264: F781–91.